

Article

A Methodology of Creating a Synthetic, Urban-Specific Weather Dataset Using a Microclimate Model for Building Energy Modelling

Mohamed H. Elnabawi ^{1,*}  and Neveen Hamza ² 

¹ Architectural Engineering Department, College of Engineering, United Arab Emirates University, Al Ain P.O. Box 13393, United Arab Emirates

² School of Architecture, Planning and Landscape, Newcastle University, Newcastle upon Tyne NE1 7RU, UK

* Correspondence: mohamedmahgoub@uaeu.ac.ae

Abstract: The relationship between outdoor microclimate and indoor building conditions requires the input of hourly weather data on the typical meteorological characteristics of the specific location. These data, known as typical meteorological year (TMY), are mainly deduced from the multi-year records of meteorological stations outside urban centres, preventing the actual complex interactions between solar radiation, wind speed, and high urban density. These factors create the urban heat island effect and higher ambient air temperatures, skewing the assumptions for energy demand in buildings. This paper presents a computational method for assessing the effect of the urban climate in the generation of typical weather data for dynamic energy calculations. As such, the paper discusses an evaluation method of pairing ENVI-met 4 microclimate and IES-VE building energy modelling software to produce a typical urban specific weather dataset (USWDs) that reflects the actual microclimatic conditions. The ENVI-met results for the outdoor microclimate conditions were employed to determine the thermal boundaries for the IES-VE, and then used to compute the building's energy consumption. The energy modelling that employed the USWDs achieved better performance compared to the TMY, as the former had just a 6% variation from the actual electricity consumption of the building compared to 15% for the latter.

Keywords: ENVI-met; energy modelling; microclimate; urban specific weather dataset (USWDs)



Citation: Elnabawi, M.H.; Hamza, N. A Methodology of Creating a Synthetic, Urban-Specific Weather Dataset Using a Microclimate Model for Building Energy Modelling. *Buildings* **2022**, *12*, 1407. <https://doi.org/10.3390/buildings12091407>

Academic Editor: Alessandro Cannavale

Received: 30 July 2022

Accepted: 6 September 2022

Published: 8 September 2022

Publisher's Note: MDPI stays neutral with regard to jurisdictional claims in published maps and institutional affiliations.



Copyright: © 2022 by the authors. Licensee MDPI, Basel, Switzerland. This article is an open access article distributed under the terms and conditions of the Creative Commons Attribution (CC BY) license (<https://creativecommons.org/licenses/by/4.0/>).

1. Introduction

It is well known that urban heat islands (UHI) arise when trapped heat is released, increasing the temperature of built-up urban areas in comparison to adjacent rural areas; this issue is due to the comparatively larger amount of incident solar energy absorbed and stored by manmade materials. This makes cities particularly vulnerable to meteorological hazards and climate change [1]. In this context, the last decade has seen the most rapid growth in energy demand, at 2.3% higher than in 2018 [2]. Much of this energy is used to create comfortable levels of heating, ventilation, and air conditioning (accounting for 35%), compared to lighting (11%) and major appliances (18%); the other 36% is spent on miscellaneous uses such as electronics. As such, the Paris Agreement reported an urgent need for reduced total energy demands and GHG emissions. In addition to the inevitable 1.5 °C increase in global temperatures, adaptation strategies are required to enhance the design of urban areas and energy systems [2]. In this regard, the Energy Performance Buildings Directive 2002/91/EC obligates all EU members to enact innovations and practices to react to the rising energy demands from the building sector [3]. However, with the current status of “climate action failure”, there is a very high risk that over the next decade there will be the most damage ever seen on a global scale [4]. In the arid climate, this problem is

even worse due to the predicted air temperature increase and the negative implications of this for ecosystems and mortality rates [5,6].

Dynamic energy simulation has therefore become a key tool in the primary phases of building designs due to its ability to represent the complex, temporary phenomena that govern a building's energy performance [7]. In the last fifty years, building energy simulation (BES) research has been focused on improving the dependability of modelling tools and since building energy consumption is weather-dependent, numerous efforts have been made to combine building energy simulation and analysis with weather datasets [8]. In this regard, weather data files are an essential input for BES as their accuracy is crucial not only for representing the external conditions around the building being modelled [9] but also for the computation of the building's heating and cooling loads [10]. Weather files for BES are an artificial climate profile comprised of averages of 25–30 years for every hour in a year. Crucially, they are gathered from weather stations often located at airfields, where there is no UHI effect. As such, if they are used to represent variations in local measured climatic conditions, this can lead to a miscalculation in the energy modelling of a building located in a dissimilar environment. That is, the building being modelled could be in an urban area with limited vegetation and isolated obstacles or a city centre with a mix of building rises [11–14]. This difference is key, as air temperatures in street canyons can typically be higher. For example, a study reported a rise of 4–6 °C in street canyons over temperatures in rural areas in Hong Kong, a high-density city [15]. This difference affects both a building's energy performance and pedestrian comfort, as well as outdoor space usage [15].

Uncertainty with weather file data in BES is high [16], and the data may also not reflect recent and future weather conditions [17]. For example, typical weather data from 1961–1990 were found to underestimate a Bahraini building's energy consumption by 14.5% in comparison to data from 1992–2005 [18]. In a sensitivity study that involved three TMY datasets and four Chinese cities, Sun et al. [19] found that building energy predictions can vary by 10% to 20%. Bourikas et al. [20] show that microclimate plays a significant impact in calculating building heating and cooling loads in the subtropical climate of Hangzhou, China. The study used actual measurements of air temperature and relative humidity at 26 sites within a 250-m radius, the outcomes show the limitations of weather datasets like the TMY, where the final heating and cooling loads computed with/without considering the microclimate showed variations of up to 20%. Furthermore, Dorer et al. [21], used a thorough building energy simulation (BES) for a typical office building in an urban canyon, local weather was found to have a significant effect on how much heat is exchanged between buildings, which in turn affects how much energy is required. In Chicago, Jain et al. [22] used the data exchange and coupling between a high-resolution microclimate model and a BES to evaluate the impact of urban weather boundary conditions on buildings' energy performance, where using a local weather dataset led to a 4.7% difference in cooling energy use compared to TMY weather data. In Montreal, Canada, a large-scale building performance simulation was performed where the findings showed discrepancies of between 3% and 29% in energy use simulated by actual and default meteorological data [23]. Another more recent study in 2021 reported an underestimation of 12.5% for peak heating load and 18% for peak cooling load in a residential building as a result of using a typical meteorological year (TMY) [16]. Therefore, it can be concluded that most existing BESs lack the ability to consider micro-scale variability in the urban microclimate, and this could significantly alter a building's energy performance in dense cities [24].

Nevertheless, the urban microclimate and UHI are influenced by the surrounding buildings and urban manmade features, which in turn alter people's outdoor thermal sensation. For this reason, urban microclimate simulation is mainly used to investigate how the built environment alters the local microclimate and outdoor thermal comfort, and it does so by influencing a series of thermodynamic phenomena [25]. The programs provide information related to microclimate performance such as air temperature (T_a), mean radiant

temperature (MRT), relative humidity (RH), thermal comfort indices, such as predicted mean vote (PMV), and wind speed. Generally, the computation domains are restricted to outside walls when the aim is solely the evaluation of the microclimate or the thermal comfort of pedestrians. Indoor profiles of use are averaged, so energy evaluation is not directly possible [26].

Although urban context design and building energy performance are interrelated and co-dependent, and despite the availability of numerous BES tools, there is no single tool which can directly evaluate the influence of an actual urban context and its microclimate on a building's energy performance, for the reasons of micro-scale variability noted above. This was concluded by Lauzet et al. [27] detailed literature review on how local climate affects building energy models in urban settings, noting that exchanging boundaries between BES and urban micro-climate models requires to be generalized to improve the accuracy of building simulations. Due to this lack of integration of climatic aspects in the planning and design process, there is an urgent need for interdisciplinary collaboration between urban planners, building designers, and urban simulation experts [28–30]. In this paper, we, therefore, present a comprehensive practice for creating a more localised weather data file for the microclimate conditions of a university campus in Manama, Bahrain in an attempt to generalize and simplify the creation of a more localized weather file. This involved a numerical simulation combining two different modelling approaches. First, ENVI-met 4 was used as a computational fluid dynamics (CFD) tool for analysing the interaction between the microclimate and a building in Manama, Bahrain; second, the BES tool IES-VE was used to calculate the building's energy performance. In so doing, it was hoped that a realistic energy consumption profile could be attained. The main objectives of this study are:

- Quantification of the interaction between the localised microclimate and a building's energy consumption
- Evaluation of the usefulness of pairing ENVI-met 4 and IES-VE as a promising approach to improving urban microclimate and reducing energy consumption in buildings in hot, arid climates.

2. Overview: Methods of Creating Typical Weather Years

In terms of simulations, the need to balance precision against computational efficiency has prompted the use of typical weather files in BES. Several approaches for acquiring typical weather data have been documented, and here we consider four methods: typical meteorological year (TMY), test reference year, meteorological year for energy calculation (MYEC), and example weather year (EWY).

In 1978, the TMY format was produced by the United States National Renewable Energy Laboratory for 248 locations, utilising long-term measurements of solar radiation and weather data from 1952–1975; it is one of the most often used hourly data format files for BES [31]. Later revisions, beginning in the early 1990s, introduced the TMY2 format, drawn from measurements taken between 1961–1990 [32] (William, 1996), and the current TMY3 datasets cover 1020 US locations using data from 1976–2005 or 1991–2005 [33]. The typical year is made up of 12 typical meteorological months [34] taken from various years and combined into a single year [35]. Gazela and Mathioulakis [36] provide a full description of how a TMY is produced. The TRY approach was established by the Chartered Institution of Building Services Engineers (CIBSE) [37], using a similar compilation procedure based on long-term measurements (generally 20 years). Finkelstein-Schafer statistics are predicted for every month and climatic variable so that typical months can be defined, and these are then aggregated to make a whole year. The full selection process for the average months that make up a TRY is described in [38]. Currently, CIBSE used the average dry bulb temperature from April to September to calculate the Design Summer Year (DSY). The simplicity of this method excludes factors like incident solar radiation and extreme monthly temperature values, both of which have a significant impact on a building's ability to withstand summer overheating. However, Jentsch et al. [39] investigated the validity of

this simplified approach which showed inconsistent relation between the DSY and the corresponding TRY and that, for some sites, building performance simulations using DSY files produce unreliable outcomes. There are two major differences between the TRY and TMY techniques: (1) in the TRY technique, only the mean values of dry bulb temperature, wind speed, and global solar radiation are considered, while the TMY method includes nine variables; and, (2) in TRY, all three variables have equal weight, but TMY uses the meteorological year for energy calculation method.

The MYEC approach was first proposed by Crow [40] as another means of producing hourly weather datasets. Although, as with TMY, the WYEC approach forms a complete year by defining 12 representative months, there are two important differences with both TRY and TMY techniques. First, a month is only chosen if the average monthly dry bulb temperature differential is ± 0.2 °C. Following the initial choice, if anomalies or extreme events are located, separate days or hours can be manipulated so that the monthly mean values are nearer to the long-term values, respectively. The entire process of creating hourly weather values, as well as further improvements to it, have been illustrated by Crow [41] and later Augustyn [42].

The last approach considered here is the EWY method of Holmes and Hitchin [43]. In this process, monthly mean weather values with the fewest anomalies compared to long-term observations are used to create an example weather year. As such, an entire representative year rather than representative months is established, as monthly mean values for global and diffuse radiation, daily mean wind speed, mean, maximum and minimum dry bulb temperature and their standard deviation from the long-term mean are predicted. Years with monthly means greater than the standard deviation from the matching long-term mean are excluded until one year remains, and this becomes the selected example year [37,44].

3. Methodology

This study presents a computational method of generating a synthetic localised urban climate weather profile for BES which reflects the influence of both the local context and site-specific microclimatic conditions. Building energy and microclimate modelling approaches were combined to assess and quantify the influence of the local microclimate on a building's energy behaviour in the hot, arid climate of Bahrain. The suggested framework is comprised of four stages (Figure 1), including two modelling programs in which IES-VE is used for the BES and ENVI-met 4 for microclimate modelling. This pairing permits the exchange of the relevant boundary conditions between the two models, with ENVI-met creating the hourly weather dataset later used in IES-VE as boundary conditions to mirror the typical meteorological phenomena of a precise site. The ENVI-met output files include the microclimatic parameters of the site around the building, and these must first be input into a weather file generator, such as Meteonorm, to produce a weather dataset compatible with being uploaded to IES-VE. As such, these data are more representative of the site being assessed and so facilitate greater accuracy with the energy modelling performance. The suggested framework is thus based on interoperability and data exchange between (Figure 1):

- a. ENVI-met v.4 microclimate model
- b. Meteonorm Weather Generator
- c. IES-VE as BES

For the case study location, we started with microclimate modelling of the current urban settings. ENVI-met modelling is time-consuming, potentially taking 24–48 h for each simulation of the model area and its resolution; for this reason, simulating every diurnal cycle for several years to produce long-term microclimatic results was too inefficient. Because of this limitation, six representative days were simulated, one for each month of the extreme summer temperatures when the cooling load is greatest (see Section 3.1). A specific urban weather dataset was then created from these microclimate results [45,46].

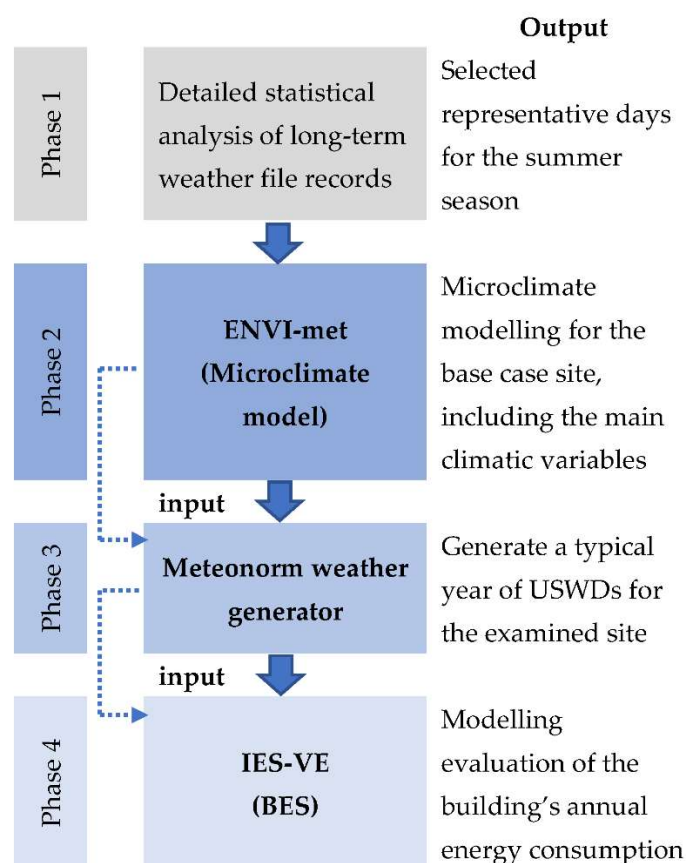


Figure 1. Methodological approach.

From the ENVI-met receptors sited around the building, a CSV (character separated values) file was collected which included the average values of air temperature, relative humidity, wind speed, and solar radiation. These were then used as inputs for Meteonorm, which can create a time series of hourly data. As such, this resolved the aforementioned limitation by generating a customised typical year file for the study location's climate, known as an urban-specific weather dataset (USWD). The precise location was identified using the 'create new location' Meteonorm map tool, and the location's situation was modified to 'centre of a large city (over 100,000 inhabitants)'; moreover, we used the clear sky radiation model and selected the output file in the EnergyPlus (epw) format. This USWD file, which is a more specific weather file that depicts the microclimate near a building, can then be input as the boundary condition in IES-VE and should improve the energy modelling performance as the real microclimate conditions for the site have been employed.

3.1. Identifying the Representative Summer Days for ENVI-Met Modelling

Tirabassi [47] stated that a representative summer day can be defined as the set of 24-h weather station data with the fewest differences from other 24-h long-term observations recorded at the same station. In the same way, Santamouris [48] proposed that a representative day illustrates a day on which the climate variables almost correspond to the long-term averages of the respective month. Thus, to define the representative days for the study modelling, long-term values for all the major climate variables were taken from the 2004–2018 database. Using air temperature as an example, the procedure for determining representative days for the microclimate simulation, as proposed by Tsoka et al. [49], was as follows:

- For each day of each month, the mean daily average air temperature was calculated, over the multi-year timeframe. For example, for 1 January and air temperature:

$$T_{\text{air 1st mean}} = (T_{\text{air aver_1st}} - 2004 + T_{\text{air aver_1st}} - 2005 + T_{\text{air aver_1st}} - 2006 + \dots + T_{\text{air aver_1st}} - 2018)/n \quad (1)$$

where, n is the number of years in the long-term period.

- For each month, the median of the previously estimated mean values was calculated. For example, for air temperature:

$$\text{Median} \{T_{\text{air 1st mean}}, T_{\text{air 2nd mean}} \dots T_{\text{air 31st mean}}\} \quad (2)$$

Following this method, the representative days were defined, followed by the microclimate simulations, to acquire the values of all the major climate variables for input to Meteorm.

3.2. The Study Context (Base Model and Location)

The Applied Science University (ASU) in Al-Ekr, south of Manama, in the Kingdom of Bahrain (26.08° N, 50.36° E) has an area of about 24,000 m² (Figure 2). It is located in a category 0B climate zone [50] and is BWh according to the Köppen-Geiger climate classification [51]. This means extremely hot summers from May to October and mild winters from November to April. As shown in Figures 2 and 3, the on-campus case study building, known as Building Technology, has a total area of 1488 m². The building's typology is a mixture of offices, classrooms, computer labs, and laboratory spaces over three floors. Its basic construction is a reinforced-concrete post and beam structure with 0.2 m thick brick infill walls which have no insulation; the building envelope is not airtight. Double-glazed windows have a visible light transmittance of 39%, and the facades are estimated to be 50% glass, with no solar protection. Table 1 provides a description of the building and the properties of its construction materials. For ground contact construction in IES-VE, the Floor-plan method was activated with the value of $U = 0.57 \text{ W/m}^2\text{-K}$. Having no heating system, the building's air-conditioning is set constantly at 21 °C so each space has been assigned as an independent thermal zone for the three floors. A lighting density of 10 W/m² and a computer load of 7 W/m² were used to represent operational hours between "8.00–17.00". Occupancy density was set as 10 m²/person in office spaces and 5 m²/person in classrooms. Daikin indoor/outdoor units have been fitted, with an energy efficiency ratio (EER) of 5 in cooling mode.



Figure 2. ASU campus, with Building Technology as the case study building.

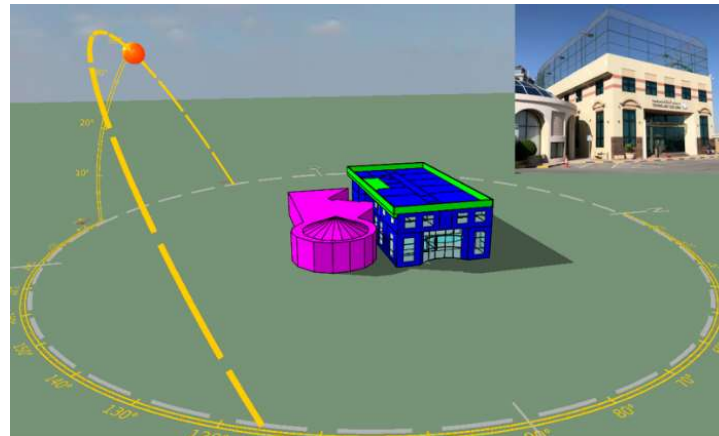


Figure 3. Building Technology's IES-VE model.

Table 1. Simulation inputs for the building's properties.

Building Properties	
Total floor area	1488 m ²
Total volume	5613 m ³
External wall area	1146 m ²
External opening area	260 m ²
External wall insulation	U-Value: 0.35 W/m ² -K
Roof insulation	U-Value: 0.35 W/m ² -K
Floor insulation	U = 0.57 W/m ² -K
Glazing	2 Dbl LoE Spec Sel Clr 6 mm/13 mm
U-Value SHGC	Arg 1.34 W/m ² -K
Light transmission	0.42 0.68
Window-to-wall ratio	50%
Shading	Blinds (inside) with high-reflectivity slats
Shading control type	Glare
Maximum allowable glare index	22

3.3. ENVI-Met Micro-Urban Modelling

With the abovementioned techniques, when generating a suitable climatic dataset, multiple years of meteorological values are required; therefore, the micro-urban modelling was conducted with the three-dimensional non-hydrostatic climate model in ENVI-met 4. This advanced simulation system is founded on the fundamental laws of thermodynamics and fluid dynamics. This software can simulate wind flow around buildings to replicate outdoor microclimatic dynamics, by handling the interplay between the climatic variables, vegetation, soil, and surface roughness [52]. Because of this advantage, the software has often been employed to perform micro-urban modelling and outdoor thermal comfort analysis in the urban canopy layer (UCL) [53–56]. The simulation grid for ASU's campus was 80 × 40 × 90, with a resolution of 2 m × 2 m × 4 m, as X, Y and Z, respectively (see Figure 4). The area of the model was rotated 5° out of the grid north to the east. Nesting grids around the main area were set at 0, and the soil profiles for these grids were set as [SD] sandy soil for soil set A, and [ST] asphalt road for soil set B. Vertical grid generation was equidistant, meaning all dz (height) were equal except for the lowest grid box. The default wall and roof properties were [00] concrete slab, and hollow block. Four snapshot

receptors were placed around the building to capture hourly the microclimatic variables that resulted from the modelling for each representative day (depicted as orange spots in Figure 4). The diurnal cycle of vertical boundary conditions was defined by air temperature, humidity, wind speed/direction, and solar radiation using the EnergyPlus weather file for each simulated day to create the full forcing boundary condition (Figure 5).

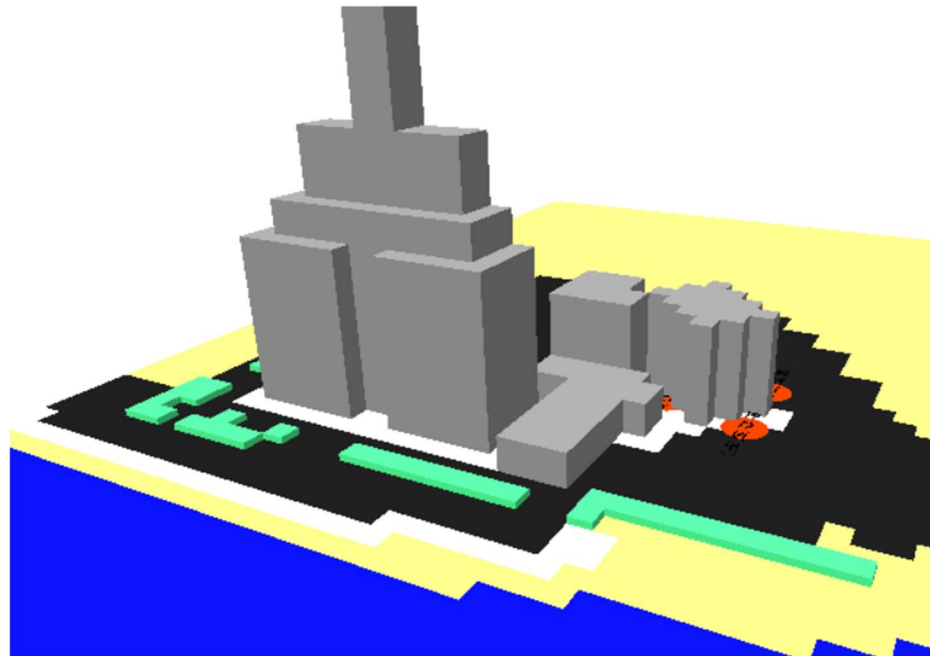


Figure 4. The ENVI-met 3D model of the ASU campus.

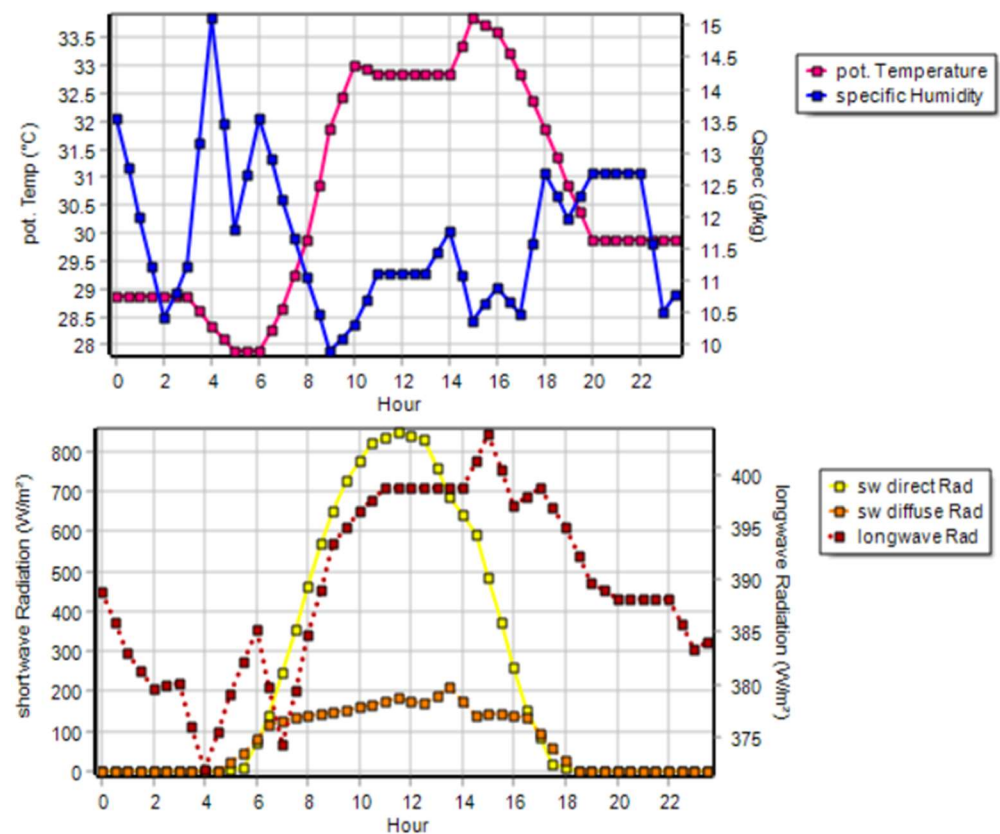


Figure 5. Cont.

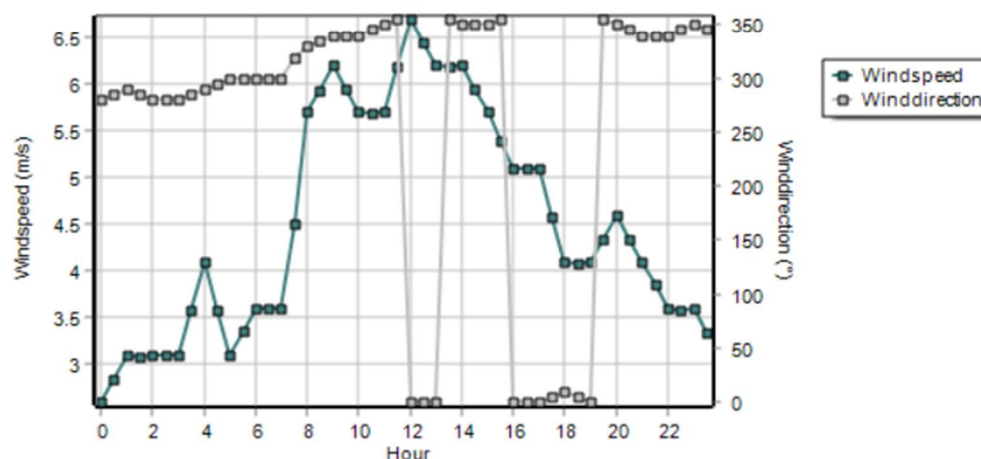


Figure 5. Full forcing boundary conditions for the ENVI-met depicting direct shortwave, diffuse shortwave, and longwave radiation (top graph), potential air temperature and specific air humidity (middle graph) as well as wind speed and wind direction (bottom graph) on the 23 May.

4. Results and Discussion

4.1. Generating Micro-Urban Specific Weather File

Data on daily average air temperature were gathered from Bahrain’s international airport weather station (no. 411500) for 2004–2018, and then analysed following the process in Tsoka et al. [49]. The main value of the daily average temperature was found for every day and month, and then divided by the total number of years for the period covered in the weather file. Then, for every month, the median of these mean values was estimated using Equations (1) and (2). Following the methodology described in Section 3.1, representative dates were determined (Table 2). ENVI-met micro-scale simulations were then performed for each of the six days that represented the summer season in Bahrain, to find the main climatic values gathered from the four receptors placed around the case study building. These values were then averaged and input as monthly data in Meteororm.

Table 2. Selected representative days in summer in Bahrain, with air temperature (T_{air}) deviations from monitored long-term median values.

Selected Representative Day	Average Air Temperature	T Air Deviation
23 May 2006	31.7	0.5%
27 June 2015	34.3	0.7%
7 July 2015	35.7	0.8%
18 August 2018	35.5	0.1%
14 September 2008	33.8	0.1%
19 October 2007	30.3	0.2%

4.2. ENVI-Met Modelling Outputs

Because of the extended calculation time required for an ENVI-met simulation, only the representative summer days shown in Table 2 were simulated. Each model was performed for 24 h, in addition to four further hours used as a spin-up stage to improve the precision of the CFD simulation. Initialising the simulation at night when turbulence conditions are weaker can reduce numerical errors or noise in the outcomes [57]. The ENVI-met output for each day’s air temperature was then compared to the values recorded for the same days from the actual data taken from Bahrain’s international airport weather station (WMO). Figure 6 shows that the ENVI-met air temperature was always greater than that actually recorded, possibly because of the dissimilar environmental conditions at each site; the meteorological station at the airport is just outside the city and occupies a different height.

Thus, the higher simulated air temperature could be accounted for by a UHI. In a similar study, the in-site monitored air temperature was 2.2 °C higher than the reported ones using the EPW in the urban centre, and the study relates this to the UHI [58]. The simulated air temperature (T_a) for the case study ranged from 33.6–39.1 °C, a greater range compared to the average measured monthly value for Bahrain (33–38 °C) recorded at the WMO. In a study by Radhi et al. [59], it was found that the air temperature in Bahrain is increasing by 1.4 °C per decade, accompanied by an increase in direct solar radiation, and as such, this is another factor to consider in simulation weather profiles. Figure 7 presents that ENVI-met relative humidity was always less than the monitored ones at the WMO yet following the same trends. Finally, using root mean square error (RMSE) as a statistical evaluation for the accuracy of the model, as shown in Table 3, it can be seen that all the outcomes fall within the acceptable range of $\pm 20\%$ [60–62].

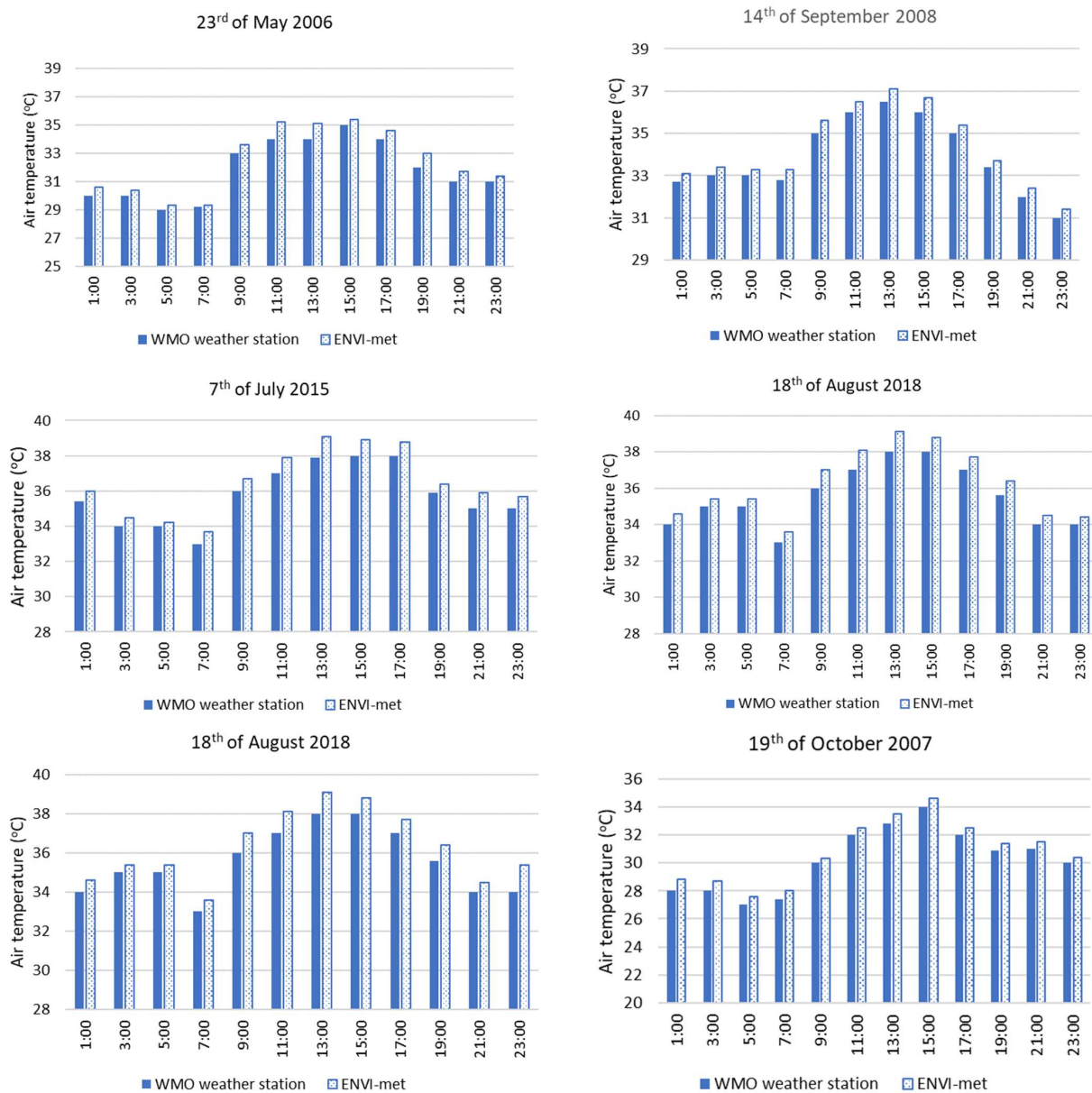


Figure 6. Variation in average air temperature reported by the WMO and the ENVI-met simulated outcomes for the representative days of summer.

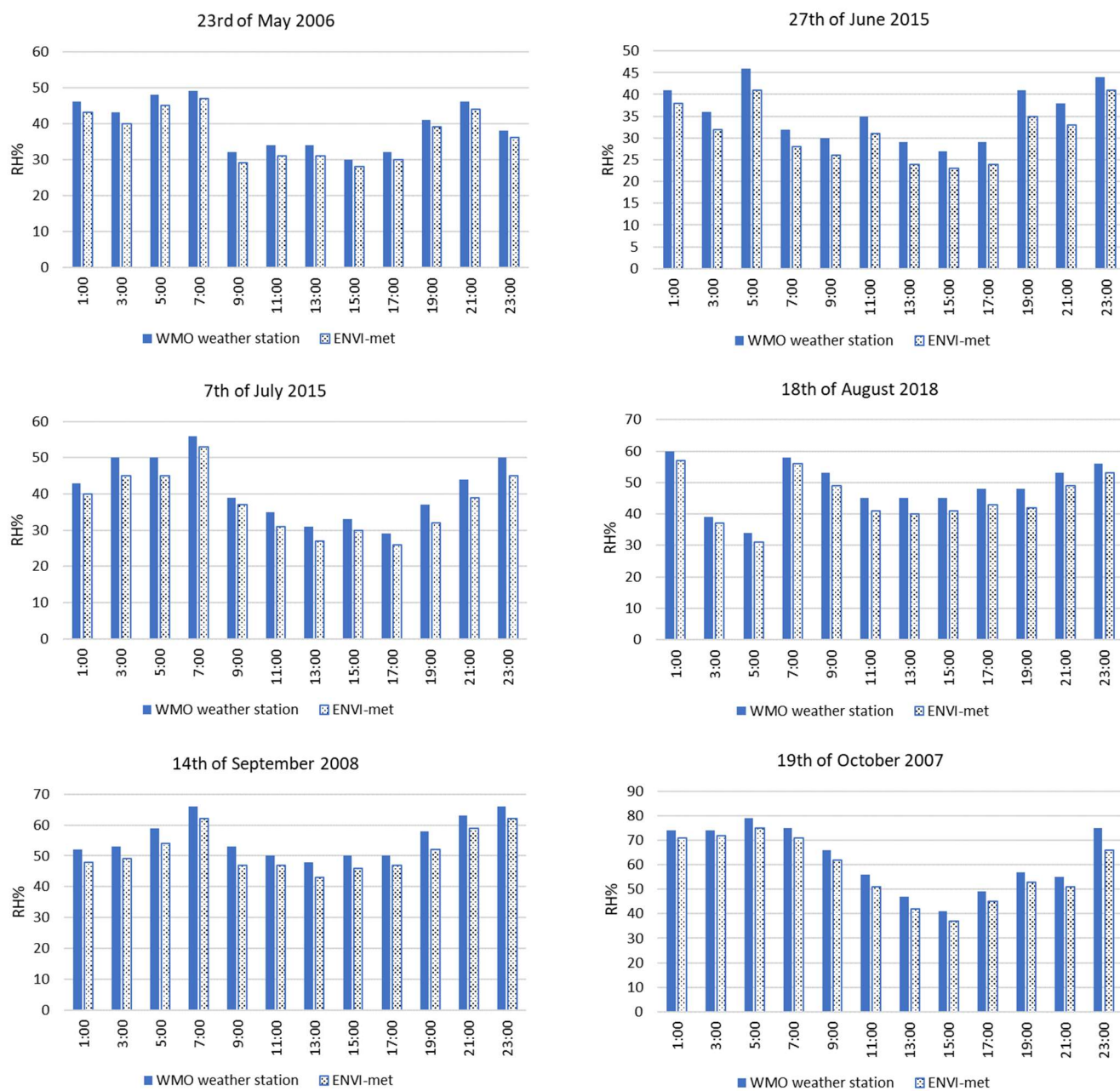


Figure 7. Variation in average relative humidity reported by the WMO and the ENVI-met simulated outcomes for the representative days of summer.

Table 3. Statistical evaluation of the Envi-met model based on RMSE.

	Average Air Temperature (°C)	RMSE	Average Relative Humidity (%)	RMSE
May	32.5	0.695	37	2.55
June	35	0.639	31	4.416
July	36.1	0.757	37	4.052
August	36.25	0.839	45	3.926
September	34.3	0.473	51	4.435
October	30.8	0.574	58	4.619

4.3. IES-VE Energy Simulation (BES)

Since the study's aim was to assess the influence of outdoor microclimate conditions on building energy performance, the microclimate weather data produced in the previous stages were then input to the building energy simulation program (BES) to compute the energy consumption of the case study building. Virtual Environment (IES-ve) version 2021, developed by the Integrated Environmental Solutions Ltd. in Glasgow, UK, is the industry standard software for thermal and comfort analysis, daylighting, solar studies, egression, and carbon emissions code compliance [63–65].

4.4. IES-VE Outcomes Using the Generated USWDs

Another study aim was to explore the validity of the paired simulation approach. As discussed, the precision of the energy modelling is determined by how accurately the input data are representative of the case study [63], which has all the complexities of reality [66]. To test the accuracy of the approach, two weather profiles were employed to simulate the same energy model in IES-VE, following European Standard EN 15603 [67] validation procedures [68]. One used the weather data from the WMO and the other an artificial USWD generated by Meteonorm based on the values gathered from the ENVI-met receptors around the case study building. The building's energy consumption for each weather profile was compared to the actual electricity metering. Figure 8 shows the IES-VE predicted total electricity consumption during summer was 595 MWh, deviating by 6% from the actual measured consumption (560 MWh). In contrast, the weather station energy simulation predicted the energy demand to be 664 MWh, with a 15% deviation against actual consumption. Regarding the accuracy of the model's predictions, RMSE for the USWD simulation was 3.5%, whereas the WMO simulation was almost twice as much at 6.6%. As such, both results are within ASHRAE 14 tolerance criteria for RMSE of $\pm 20\%$ [60–62]. From this, it can be deduced that creating localised urban boundary conditions for a building decreases variation in estimated building energy demands.

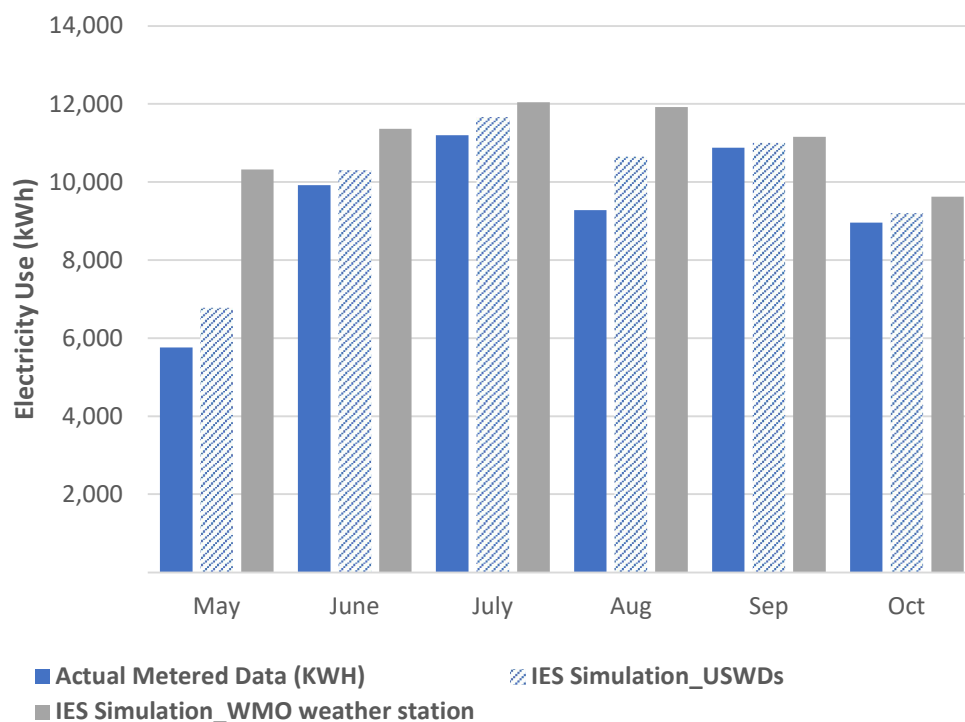


Figure 8. Actual electricity consumption v. IES-VE simulated, using USWDs and WMO data.

The building energy model employed occupancy profiles which were as near to actual recorded occupancy levels as possible, although they may appear to be much higher than the simulation outcomes. This might be because of the building type and its

variable occupancy schedule, which follows the academic calendar and university teaching periods. In general, the monthly electricity consumption seen with both IES-VE models was reasonably distributed with regard to the corresponding monthly actual values, although as we have seen the USWD model deviated less from the actual energy bills, with a deviation of 6% against 15% for the WMO energy model. Nevertheless, both outcomes correlate strongly to the measured consumption and are within the accepted range of deviation of <10–20% [69,70].

These outcomes are aligned with other findings from different studies such as Tsoka et al. (2018) [49] who indicated mean daily deviations reaching between 0.63 °C and 1.0 °C and Fan et al. (2020) who reported an increase from 0.1 °C to 1.3 °C in the outdoor air temperature which has an impact on building energy loads, as per the findings of Santamouris et al. [71] literature review, which suggest an increase in the peak energy load ranges between 0.45% and 4.6% per degree of air temperature increase, whereas the comparative analysis of existing scientific results reported 13% average cooling load increase according to the severity of the phenomena and the characteristics of the buildings [71]. This might be one of the reasons explaining the outcome variation among the different studies, where variations of up to 20% were observed in the final heating and cooling loads when considering the microclimate [20]. Very similar outcomes were reported by Sun et al. [19] in four cities in China with 10% to 20% variation in building energy calculations based on sensitivity analysis using different TMY files. While using a local weather dataset led to a 4.7% difference in cooling load in Chicago compared to TMY weather data [22]. In a more detailed recent study investigating the TMY impact on building energy performance in six different cities in China, the relative mean deviation, the results show a total 0.7–10% difference [72].

4.5. ENVI-Met Modelling Outputs for an Improved USWD

To improve understanding of the link between outdoor urban design and indoor energy consumption, simple outdoor passive design interventions have been suggested to exploit the advantageous aspects of climatic conditions, including outdoor air temperature and its significant influence on a building's energy balance. Outside air temperature affects heat transfer through external walls and roofing, as well as heat transfer through ventilation [73]. Additionally, outdoor relative humidity is key in hot seasons [74] as it has a significant effect on latent cooling load and energy consumption in summer. When investigating condensation conditions, the year-round external air humidity must be taken into consideration [73]. In this regard, the presence of suitable vegetation at a site is one possible design intervention which can regulate outdoor air temperature and relative humidity [74,75]. Accordingly, the car park was replaced with green spaces, in which grass was set to be 50 cm high to avoid wind obstruction. Figure 9 presents the current and amended scenarios.

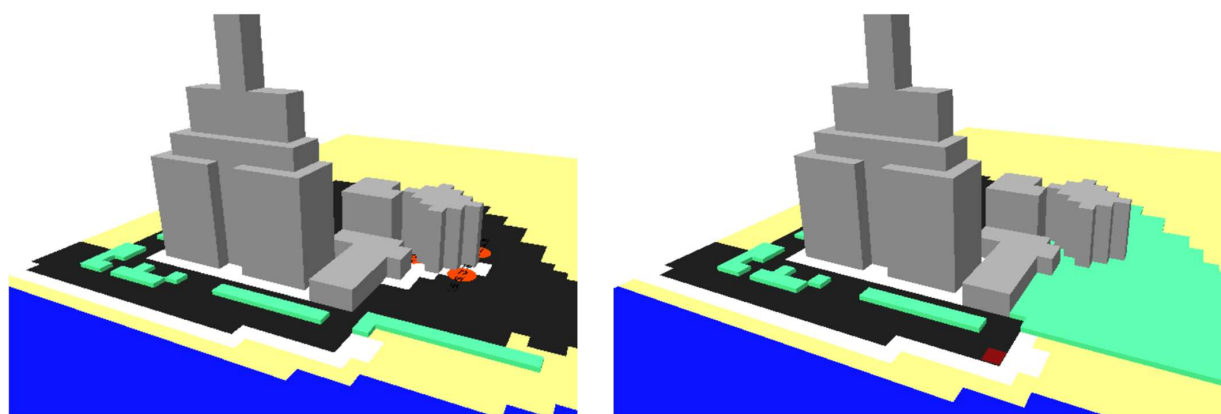


Figure 9. The existing base case with hard surfaces (left) and the amended scenario with green spaces (right).

Using the previous settings for the ENVI-met simulation, only the six days representing the summer season (Table 2) were simulated, to generate a USWD for the amended scenario to represent the impact of the intervention on the climatic conditions. Again, the main climatic values taken from the four receptors around the case study building were averaged and used as monthly data input for Meteonorm. Figures 10 and 11 illustrate the difference in air temperature and relative humidity between the existing and amended case study scenarios. In Figure 10, the air temperature showed the same drift with lower values as the base case during the whole day for all the summer months. The proposed intervention led to an average of 0.6 °C lower than the base case. May recorded the highest difference of 0.78 °C, followed by 0.67 °C for August, while the least difference was seen in June and July, at 0.49 °C and 0.42 °C, respectively.

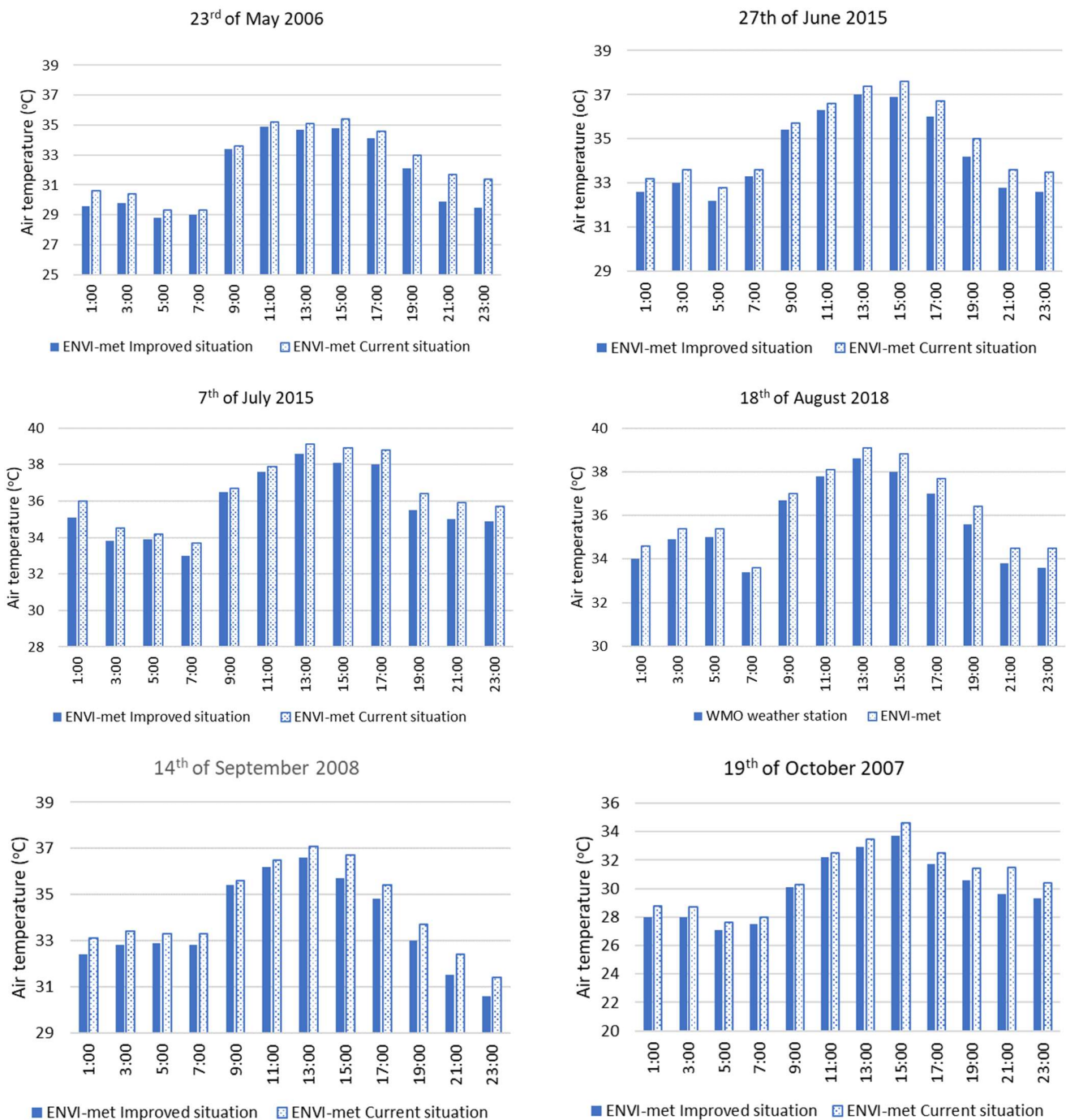


Figure 10. Comparison of average air temperature for the existing v. amended case study.

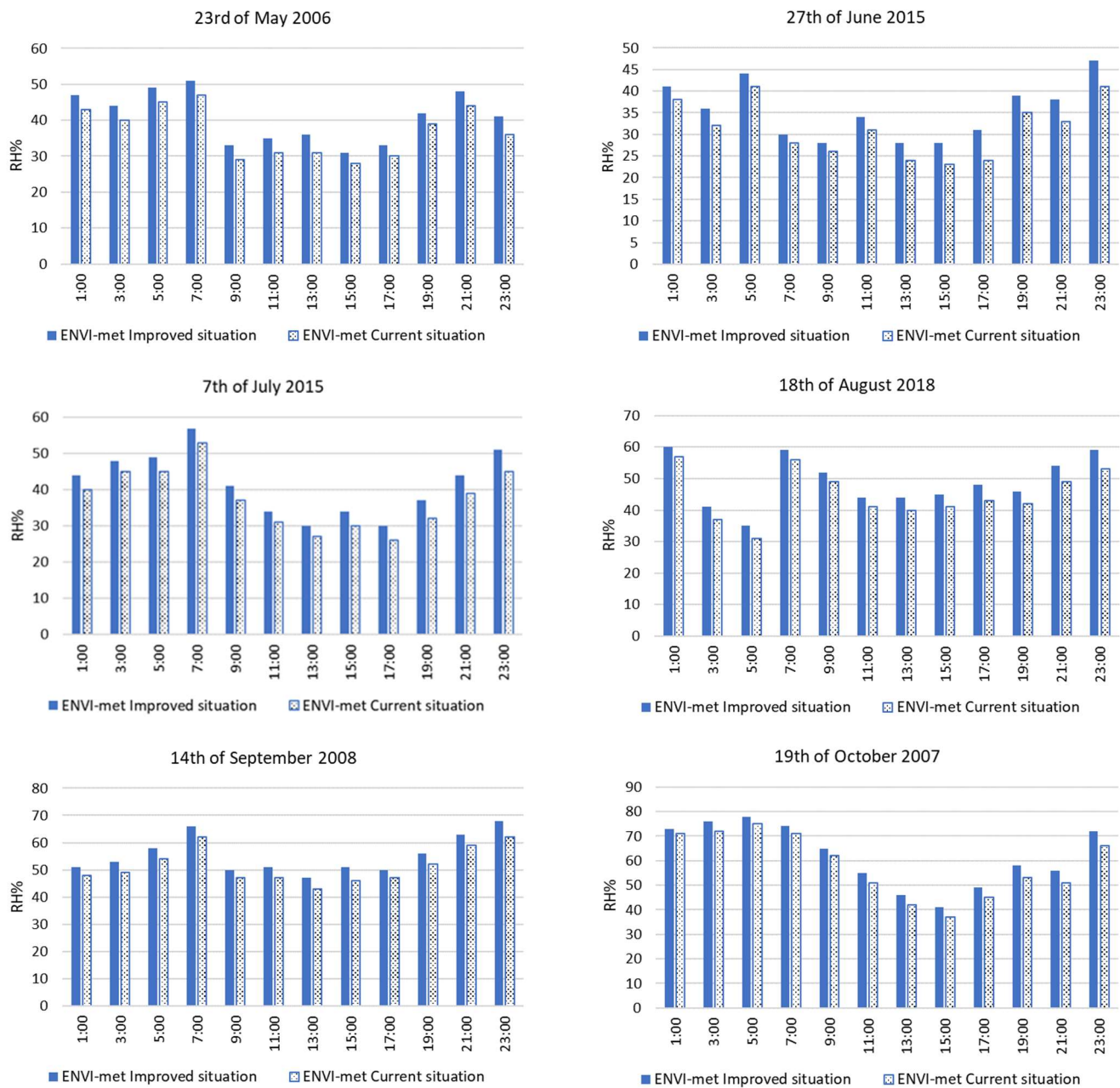


Figure 11. Comparison of the average relative humidity (RH) for the existing v. amended case study.

Figure 11 shows that the relative humidity of the amended case increased by an average of 4% compared to the base. The lower air temperature and higher relative humidity outcomes are due to the addition of more green area in the urban spaces, caused by its ability to convert solar radiation into latent heat, which in turn lowers the surface temperature; this is in addition to evapotranspiration, as the green spaces increase relative humidity through transpiration and wet substrate [76]. According to Yu [77], the solar radiation reaching the surface of green spaces is converted into biomass, oxygen, and humidity. Similar outcomes have been reported in previous studies. In Egypt, air temperature decreased by 1 °C and relative humidity increased by about 3% in the hot climate [74]. In Algeria, a reduction of 0.8 °C was seen in average air temperature due to the presence of more vegetation cover at the studied site [78]. Moreover, in Algeria, a comparison of empty and vegetated spaces revealed a maximum deviation between two air temperatures equal to 6.57 °C, and higher relative humidity for the vegetated area with a difference

of 0.4 g/kg [75]. In Gothenburg, Sweden, during summer the average difference in air temperature was about 3 °C in the park compared to the surrounding neighbourhood [79].

4.6. IES-VE Outcomes Using an Improved USWDs

The two synthetic USWDs created in Meteonorm for the base case and amended scenario were also used to quantify the relationship between the local microclimate and the case study building's energy consumption. The same adjustment employed for the validation of the generated USWD was used to simulate another energy model using IES-VE. The building's energy consumption figures for both USWD weather profiles were compared. As shown in Figure 12, the IES-VE predicted total electricity consumption for the base case was 595 MWh, while the energy simulation in the amended scenario was 552 MWh, using 7.25% less total energy. This reduction may be due to the 0.6 °C average reduction in external air temperature, which could decrease the cooling load by 7.25% in summer. A similar finding was reported in previous research, in that for each 1 °C rise in outdoor air temperatures, the peak cooling load increases by approximately 10% [80].

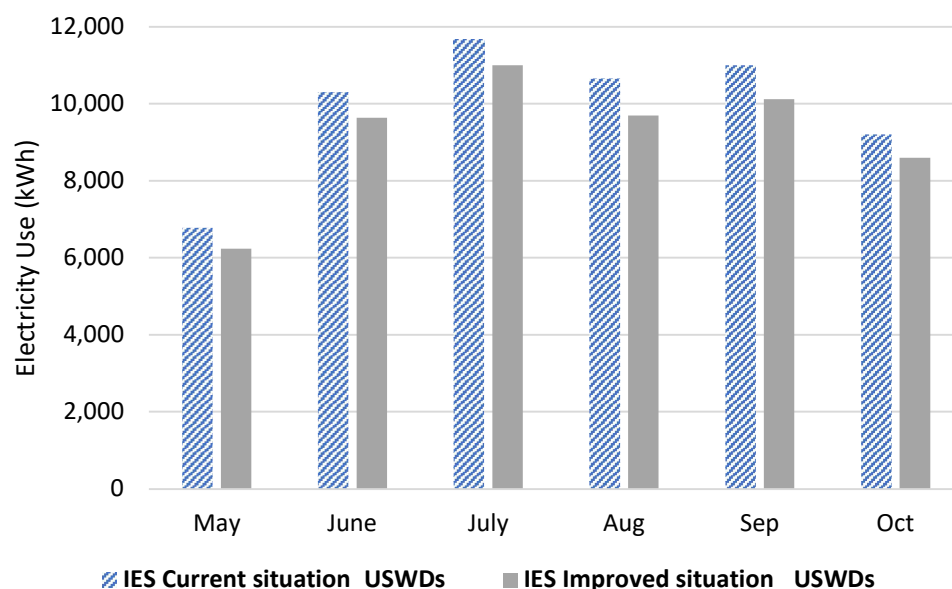


Figure 12. Comparison of the electricity consumption of the IES-VE using USWDs for the base case v. USWDs for the amended case.

5. Conclusions

Long-term local and urban environmental monitoring for the purposes of creating a climatic weather profile for building simulation is costly and complex. In this paper, the aim was to explore the feasibility of a method of creating a synthetic urban local specific weather dataset (USWD) for the estimation of energy demand. Buildings in hot arid climates, especially those with year-round occupancy, consume a great deal of energy and have large air conditioning systems. The proposed method involved using data in CSV file format exported from receptors placed at the case study building, in order to create a Metronorm urban weather profile, which could then be used to generate a yearly energy plus weather format (EPW) weather profile compatible with IES-VE (Figure 2). The key results of this assessment are:

- The method may help with the development of guidelines that link outdoor urban design with indoor building energy consumption;
- A comparison of the ENVI-met simulated air temperature and the WMO recorded datasets showed the influence of a UHI, as the simulated air temperature for the case study varied more than the average monthly value recorded by the WMO weather station at Bahrain international airport;

- The creation of a localised weather file (USWD) for BES produces data which are nearer to actual energy demand figures, with discrepancies of 6% deviation in comparison to 15% for the energy model that used the WMO weather file. Local microclimate fluctuates according to the boundary conditions, such as vegetation, surface materials, urban density, and air quality; all these influence the energy balance of buildings [12,13];
- While both IES-VE simulation outputs were within the accepted <10–20% of actual energy demand [69,70], various outdoor microclimate situations, such as the presence of certain types of vegetation, waterbodies, or surface materials should be explored with USWD files that can accurately estimate the influence on indoor energy demand;
- The site of a weather station and the date of the weather data file played a key role in the BES outcomes in this study, as seen in the variation in the USWD and WMO findings. This is in line with a previously reported outcome in a 15-year data comparison which revealed a difference of up to 3.7 °C for air temperature and 1.5 m/s in average wind velocity [16]. Similarly, another study compared two datasets from 1961–1990 and 1992–2005 and found a 14.5% discrepancy in energy analysis [18];
- The amended scenario of substituting asphalt for 50 cm high grass led to an average 0.6 °C lower outdoor air temperature and 4% increase in relative humidity against the base case. These changes, as well as other microclimate parameters, were recorded by ENVI-met receptors around the building and used to generate a new USWD for the intervention;
- IES-VE predicted that the total electricity consumption during the summer, using the USWD of the base case, was 595 MWh, whereas the energy simulation with the USWD of the amended scenario was 552 MWh, a reduction of 7.25% in total energy; in a similar study in Chicago, it was found that using a local weather dataset led to a 4.7% difference in cooling energy use compared to TMY weather data [22];
- In future research, monitored building base loads and occupancy for longer periods might reduce these discrepancies even more. Long-term on-site observation of the microclimatic parameters for comparison with ENVI-met output would further raise confidence in the paper-adopted approach.

Author Contributions: Conceptualization, M.H.E. and N.H.; methodology, M.H.E. and N.H.; software, M.H.E.; validation, M.H.E.; formal analysis, M.H.E. and N.H.; investigation, M.H.E.; data curation, M.H.E.; writing—original draft preparation, M.H.E.; writing—review and editing, M.H.E. and N.H. All authors have read and agreed to the published version of the manuscript.

Funding: This research received no external funding.

Data Availability Statement: Not applicable.

Conflicts of Interest: The authors declare no conflict of interest.

References

1. Masson, V.; Lemonsu, A.; Hidalgo, J.; Voogt, J. Urban climates and climate change. *Annu. Rev. Environ. Resour.* **2020**, *45*, 411–444. [CrossRef]
2. Intergovernmental Panel on Climate Change (IPCC). Global Warming of 1.5 °C: Special Report. 2018. Available online: https://www.ipcc.ch/site/assets/uploads/sites/2/2019/06/SR15_Summary_Volume_Low_Res.pdf (accessed on 17 October 2021).
3. Bio Intelligence Service, Ronan Lyons and IEEP. Energy Performance Certificates in Buildings and Their Impact on Transaction Prices and Rents in Selected EU Countries, Final Report Prepared for European Commission (DG Energy). 2013. Available online: https://ec.europa.eu/energy/sites/ener/files/documents/20130619-energy_performance_certificates_in_buildings.pdf (accessed on 29 July 2022).
4. The Global Risks Report 2022, 17th Edition Published by the World Economic Forum. ISBN 978-2-940631-09-4. Available online: https://www3.weforum.org/docs/WEF_The_Global_Risks_Report_2022.pdf (accessed on 15 July 2022).
5. Adam-Poupart, A.; Labrèche, F.; Smargiassi, A.; Duguay, P.; Busque, M.A.; Gagné, C.; Rintamäki, H.; Kjellstrom, T.; Zayed, J. Climate change and Occupational Health and Safety in a temperate climate: Potential impacts and research priorities in Quebec, Canada. *Ind. Health* **2013**, *51*, 68–78. [CrossRef] [PubMed]
6. Tibbetts, J.H. Air quality and climate change: A delicate balance. *Environ. Health Perspect.* **2015**, *123*, A148–A153. [CrossRef]
7. De Wilde, P. *Building Performance Analysis*, 1st ed.; Wiley-Blackwell: Oxford, UK, 2018.

8. Lazos, D.; Sproul, A.B.; Kay, M. Optimisation of energy management in commercial buildings with weather forecasting inputs: A review. *Renew. Sustain. Energy Rev.* **2014**, *39*, 587–603. [[CrossRef](#)]
9. Zhao, H.; Magoulès, F. A review on the prediction of building energy consumption. *Renew. Sustain. Energy Rev.* **2012**, *16*, 3586–3592. [[CrossRef](#)]
10. Yoshino, H.; Hong, T.; Nord, N.; Annex, I.E. IEA EBC annex 53: Total energy use in buildings—Analysis & evaluation methods. *Energy Build.* **2007**, *152*, 124–136.
11. Yang, X.; Zhao, L.; Bruse, M.; Meng, Q. An integrated simulation method for building energy performance assessment in urban environments. *Energy Build.* **2012**, *54*, 243–251. [[CrossRef](#)]
12. Ignatius, M.; Wong, N.H.; Jusuf, S.K. The significance of using local predicted temperature for cooling load simulation in the tropics. *Energy Build.* **2016**, *118*, 57–69. [[CrossRef](#)]
13. Castaldo, V.L.; Pisello, A.L.; Pigliautile, I.; Piselli, C.; Cotana, F. Microclimate and air quality investigation in historic hilly urban areas: Experimental and numerical investigation in central Italy. *Sustain. Cities Soc.* **2017**, *33*, 27–44. [[CrossRef](#)]
14. Gobakis, K.; Kolokotsa, D. Coupling building energy simulation software with microclimatic simulation for the evaluation of the impact of urban outdoor conditions on the energy consumption and indoor environmental quality. *Energy Build.* **2017**, *157*, 101–115. [[CrossRef](#)]
15. Huang, J.; Zhou, C.; Zhuo, Y.; Xu, L.; Jiang, Y. Outdoor Thermal Environments and Activities in Open Space: An Experiment Study in Humid Subtropical Climates. *Build. Environ.* **2016**, *103*, 238–249. [[CrossRef](#)]
16. Evola, G.; Costanzo, V.; Infantone, M.; Marletta, L. Typical-year and multi-year building energy simulation approaches: A critical comparison. *Energy* **2021**, *219*, 119591. [[CrossRef](#)]
17. Siu, C.Y.; Liao, Z. Is building energy simulation based on TMY representative: A comparative simulation study on doe reference buildings in Toronto with typical year and historical year type weather files. *Energy Build.* **2020**, *211*, 109760. [[CrossRef](#)]
18. Radhi, H. A comparison of the accuracy of building energy analysis in Bahrain using data from different weather periods. *Renew. Energy* **2009**, *34*, 869–875. [[CrossRef](#)]
19. Sun, J.; Li, Z.; Xiao, F. Analysis of Typical Meteorological Year selection for energy simulation of building with daylight utilization. *Procedia Eng.* **2017**, *205*, 3080–3087. [[CrossRef](#)]
20. Bourikas, L.; James, P.A.B.; Bahaj, A.S.; Jentsch, M.F.; Shen, T.; Chow, D.H.C.; Darkwa, J. Transforming typical hourly simulation weather data files to represent urban locations by using a 3D urban unit representation with micro-climate simulations. *Future Cities Environ.* **2016**, *2*, 7. [[CrossRef](#)]
21. Dorer, V.; Allegrini, J.; Orehounig, K.; Moonen, P.; Upadhyay, G.; Kämpf, J.; Carmeliet, J. Modeling the urban microclimate and its impact on energy demand of buildings and buildings clusters. Empa, Laboratory for Building Science and Technology, Solar. In Proceedings of the 13th Conference of International Building Performance Simulation Association, Chambéry, France, 26–28 August 2013; pp. 3483–3489.
22. Jain, R.; Luo, X.; Sever, G.; Hong, T.; Catlett, C. Representation and evolution of urban weather boundary conditions in downtown Chicago. *J. Build. Perform. Simul.* **2018**, *13*, 1–14. [[CrossRef](#)]
23. Hosseini, M.; Lee, B.; Vakili, S. Energy performance of cool roofs under the impact of actual weather data. *Energy Build.* **2017**, *145*, 284–292. [[CrossRef](#)]
24. Huang, J.; Jones, P.; Zhang, A.; Peng, R.; Li, X.; Chan, P. Urban Building Energy and Climate (UrBEC) simulation: Example application and field evaluation in Sai Ying Pun, Hong Kong. *Energy Build.* **2019**, *207*, 109580. [[CrossRef](#)]
25. Albdour, M.S.; Baranyai, B. An overview of microclimate tools for predicting the thermal comfort, meteorological parameters and design strategies in outdoor spaces. *Pollack Period.* **2019**, *14*, 109–118. [[CrossRef](#)]
26. Bouyer, J.; Inard, C.; Musy, M. Microclimatic coupling as a solution to improve building energy simulation in an urban context. *Energy Build.* **2011**, *43*, 1549–1559. [[CrossRef](#)]
27. Lauzet, N.; Rodler, A.; Musy, M.; Azam, M.H.; Guernouti, S.; Mauree, D.; Colinart, T. How building energy models take the local climate into account in an urban context—A review. *Renew. Sustain. Energy Rev.* **2019**, *116*, 109390. [[CrossRef](#)]
28. Nouri, A.S.; Costa, J.P.; Santamouris, M.; Matzarakis, A. Approaches to outdoor thermal comfort thresholds through public space design: A review. *Atmosphere* **2018**, *9*, 108. [[CrossRef](#)]
29. Shooshtarian, S.; Rajagopalan, P.; Sagoo, A. A comprehensive review of thermal adaptive strategies in outdoor spaces. *Sustain. Cities Soc.* **2018**, *41*, 647–665. [[CrossRef](#)]
30. Elnabawi, M.H.; Hamza, N. A Behavioural Analysis of Outdoor Thermal Comfort: A Comparative Analysis between Formal and Informal Shading Practices in Urban Sites. *Sustainability* **2020**, *12*, 9032. [[CrossRef](#)]
31. Hall, I.J.; Prairie, R.; Anderson, H.; Boes, E. *Generation of a Typical Meteorological Year*; Sandia Labs: Albuquerque, NM, USA, 1978.
32. William, M.; Urban, K. *User's Manual for TMY2S*; National Renewable Energy Laboratory: Golden, CO, USA, 1996. Available online: http://rredc.nrel.gov/solar/old_data/nsrdb/tmy2 (accessed on 20 October 2021).
33. Wilcox, S.; Marion, W. *Users Manual for TMY3 Data Sets*; National Renewable Energy Laboratory: Golden, CO, USA, 2008.
34. McLeod, R.S.; Hopfe, C.J.; Rezgui, Y. A proposed method for generating high resolution current and future climate data for Passivhaus design. *Energy Build.* **2012**, *55*, 81–493. [[CrossRef](#)]
35. Finkelstein, J.M.; Schafer, R.M. Improved goodness-of-fit tests. *Biometrika* **1971**, *58*, 641–645. [[CrossRef](#)]
36. Gazela, M.; Mathioulakis, E. A new method for typical weather data selection to evaluate long-term performance of solar energy systems. *Sol. Energy* **2001**, *70*, 339–348. [[CrossRef](#)]

37. Ozdenefe, M.; Dewsbury, J. Simulation and real weather data: A comparison for Cyprus case. *Build. Serv. Eng. Res. Technol.* **2016**, *37*, 288–297. [[CrossRef](#)]
38. Levermore, G.J.; Parkinson, J.B. Analyses and algorithms for new Test Reference Years and Design Summer Years for the UK. *Build. Serv. Eng. Res. Technol.* **2006**, *27*, 311–325. [[CrossRef](#)]
39. Jentsch, M.F.; Levermore, G.J.; Parkinson, J.B.; Eames, M.E. Limitations of the CIBSE design summer year approach for delivering representative near-extreme summer weather conditions. *Build. Serv. Eng. Res. Technol.* **2014**, *35*, 155–169. [[CrossRef](#)]
40. Crow, L.W. Development of hourly data for weather year for energy calculations (WYEC), including solar data, at 21 stations throughout the US. *ASHRAE Trans.* **1981**, *87*, 896–900.
41. Crow, L.W. Weather year for energy calculations. *ASHRAE J.* **1984**, *26*, 5758650.
42. Augustyn, J.R. WYEC2 user's manual and software toolkit. *ASHRAE Trans.* **1998**, *104*, 32.
43. Holmes, M.; Hitchin, E. An example year for the calculation of energy demand in buildings. *Build. Serv. Eng.* **1978**, *45*, 186–189.
44. Wong, W.; Ngan, K. Selection of an “example weather year” for Hong Kong. *Energy Build.* **1993**, *19*, 313–316. [[CrossRef](#)]
45. Skelhorn, C.; Lindley, S.; Levermore, G. The impact of vegetation types on air and surface temperatures in a temperate city: A fine scale assessment in Manchester, UK. *Landsc. Urban Plan.* **2014**, *121*, 129–140. [[CrossRef](#)]
46. Chow, W.T.; Brazel, A.J. Assessing xeriscaping as a sustainable heat island mitigation approach for a desert city. *Build. Environ.* **2012**, *47*, 170–181. [[CrossRef](#)]
47. Tirabassi, T.; Nasseti, S. The representative day. *Atmos. Environ.* **1999**, *33*, 2427–2434. [[CrossRef](#)]
48. Santamouris, M. *Advances in Building Energy Research*; Earthscan: Oxford, UK, 2012.
49. Tsoka, S.; Tolika, K.; Theodosiou, T.; Tsikaloudaki, K.; Bikas, D. A method to account for the urban microclimate on the creation of ‘typical weather year’ datasets for building energy simulation, using stochastically generated data. *Energy Build.* **2018**, *165*, 270–283. [[CrossRef](#)]
50. American Society of Heating. *2009 ASHRAE Handbook: Fundamentals*; American Society of Heating: Atlanta, GA, USA, 2009.
51. Peel, M.C.; Finlayson, B.L.; McMahon, T.A. Updated world map of the Köppen-Geiger climate classification. *Hydrol. Earth Syst. Sci.* **2007**, *11*, 1633–1644. [[CrossRef](#)]
52. Spangenberg, J.; Shinzato, P.; Johansson, E.; Durate, D. Simulation of the influence of vegetation on microclimate and thermal comfort in the city of Sao Paulo. *Rev. Soc. Bras. Arborização Urbana* **2008**, *3*, 1–19.
53. Tsoka, S.; Tsikaloudaki, K.; Theodosiou, T. Coupling a Building Energy Simulation Tool with a Microclimate Model to Assess the Impact of Cool Pavements on the Building's Energy Performance Application in a Dense Residential Area. *Sustainability* **2019**, *11*, 2519. [[CrossRef](#)]
54. Yang, S.-R.; Lin, T.-P. An integrated outdoor spaces design procedure to relieve heat stress in hot and humid regions. *Build. Environ.* **2016**, *99*, 149–160. [[CrossRef](#)]
55. Roth, M.; Lim, V.H. Evaluation of canopy-layer air and mean radiant temperature simulations by a microclimate model over a tropical residential neighbourhood. *Build. Environ.* **2016**, *112*, 177–189. [[CrossRef](#)]
56. Elnabawi, M.H.; Hamza, N.; Dudek, S. Use and evaluation of the ENVI-met model for two different urban forms in Cairo, Egypt: Measurements and model simulations. In Proceedings of the 13th Conference of International Building Performance Simulation Association, Chambéry, France, 25–28 August 2013.
57. Zhang, A.; Bokel, R.; van den Dobbela, A.; Sun, Y.; Huang, Q.; Zhang, Q. An integrated school and schoolyard design method for summer thermal comfort and energy efficiency in Northern China. *Build. Environ.* **2017**, *124*, 369–387. [[CrossRef](#)]
58. Wang, W.; Li, S.; Guo, S.; Ma, M.; Feng, S.; Bao, L. Benchmarking urban local weather with long-term monitoring compared with weather datasets from climate station and EnergyPlus weather (EPW) data. *Energy Rep.* **2021**, *7*, 6501–6514. [[CrossRef](#)]
59. Radhi, H.; Sharples, S.; Assem, E. Impact of urban heat islands on the thermal comfort and cooling energy demand of artificial islands—A case study of AMWAJ Islands in Bahrain. *Sustain. Cities Soc.* **2015**, *19*, 310–318. [[CrossRef](#)]
60. Hong, T.; Kim, J.; Jeong, J.; Lee, M.; Ji, C. Automatic calibration model of a building energy simulation using optimization algorithm. *Energy Procedia* **2017**, *105*, 3698–3704. [[CrossRef](#)]
61. Cipriano, J.; Mor, G.; Chemisana, D.; Pérez, D.; Gamboa, G.; Cipriano, X. Evaluation of a multi-stage guided search approach for the calibration of building energy simulation models. *Energy Build.* **2015**, *87*, 370–385. [[CrossRef](#)]
62. Kim, J.; Hong, T.; Koo, C.W. Economic and environmental evaluation model for selecting the optimum design of green roof systems in elementary schools. *Environ. Sci. Technol.* **2012**, *46*, 8475–8483. [[CrossRef](#)] [[PubMed](#)]
63. Elnabawi, M.H. Building Information Modeling-Based Building Energy Modeling: Investigation of Interoperability and Simulation Results. *Front. Built. Environ.* **2020**, *6*, 573971. [[CrossRef](#)]
64. Annan, G.; Ghaddar, N.; Ghali, K. Natural ventilation in Beirut residential buildings for extended comfort hours. *Int. J. Sustain. Energy* **2014**, *35*, 996–1013. [[CrossRef](#)]
65. Azhar, S.; Brown, J. BIM for sustainability analyses. *Int. J. Constr. Educ. Res.* **2009**, *5*, 276–292. [[CrossRef](#)]
66. Blocken, B.; Janssen, W.D.; van Hoo, T. CFD simulation for pedestrian wind comfort and wind safety in urban areas: General decision framework and case study for the Eindhoven University campus. *Environ. Model. Softw.* **2012**, *30*, 15–34. [[CrossRef](#)]
67. *DS/EN 15603:2008; Energy Performance of Buildings—Overall Energy Use and Definition of Energy Ratings*. Slovenian Institute for Standardization: Ljubljana, Slovenia, 2008.
68. *BS EN ISO 13790:2008; Energy Performance of Buildings—Calculation of Energy Use for Space Heating and Cooling*. ISO: Geneva, Switzerland, 2008.

69. Maamari, F.; Andersen, M.; de Boer, J.; Carroll, W.; Dumortier, D.; Greenup, P. Experimental validation of simulation methods for bi-directional transmission properties at the daylighting performance level. *Energy Build.* **2016**, *38*, 878–889. [[CrossRef](#)]
70. Oleiwi, M.Q.; Mohamed, M.F.; Sulaiman, M.K.A.M.; Che-Ani, A.I.; Raman, S.N. Thermal environment accuracy investigation of integrated environmental solutions-virtual environment (IESVE) software for double-story house simulation in malaysia. *J. Eng. Appl. Sci.* **2019**, *14*, 3659–3665. [[CrossRef](#)]
71. Santamouris, M. Regulating the damaged thermostat of the cities—Status, impacts and mitigation challenges. *Energy Build.* **2015**, *91*, 43–56. [[CrossRef](#)]
72. Fan, X.; Bin, C.; Changfeng, F.; Lingyun, L. Research on the Influence of Abrupt Climate Changes on the Analysis of Typical Meteorological Year in China. *Energies* **2020**, *13*, 6531. [[CrossRef](#)]
73. Goodfellow, H.D.; Wang, Y. *Industrial Ventilation Design Guidebook*, 2nd ed.; Academic Press: Cambridge, MA, USA, 2021; ISBN 9780128166734. Available online: <https://www.sciencedirect.com/science/article/pii/B9780128166734000134> (accessed on 29 July 2022). [[CrossRef](#)]
74. Barakat, A.; Ayad, H.; El-Sayed, Z. Urban Design in Favor of Human Thermal Comfort for Hot Arid Climate Using Advanced Simulation Methods. *Alex. Eng. J.* **2017**, *56*, 533–543. [[CrossRef](#)]
75. Boukhabla, M.; Alkama, D. Impact of Vegetation on Thermal Conditions Outside, Thermal Modeling of Urban Microclimate, Case Study: The Street of the Republic, Biskra. *Energy Procedia* **2012**, *18*, 73–84. [[CrossRef](#)]
76. Chen, A.; Yao, X.A.; Sun, R.; Chen, L. Effect of urban green patterns on surface urban cool islands and its seasonal variations. *Urban For. Urban Green.* **2014**, *13*, 646–654. [[CrossRef](#)]
77. Yu, M.V.D.C. *Biotechnologies and Biomimetics for Civil Engineering*; Springer: Cham, Switzerland, 2015.
78. Sayad, B.; Alkama, D.; Rebhi, R.; Menni, Y.; Ahmad, H.; Inc, M.; Sharifpur, M.; Lorenzini, G.; Azab, E.; Elnaggar, A.Y. Outdoor Thermal Comfort Optimization through Vegetation Parameterization: Species and Tree Layout. *Sustainability* **2021**, *13*, 11791. [[CrossRef](#)]
79. Upmanis, H. Daytime summer temperature differences between a green area and its build-up surroundings in a high latitude city. In Proceedings of the Second Urban Environment Symposium and 13th Conference on Biometeorology and Aerobiology, Albuquerque, NM, USA, 2–6 November 1998; American Meteorology Society: Boston, MA, USA, 1998; p. 210.
80. Watkins, R.; Levermore, G. Quantifying the effects of climate change and risk level on peak load design in buildings. *Build. Serv. Eng. Res. Technol.* **2011**, *32*, 9–19. [[CrossRef](#)]